Original Research Article

FRET based biosensor from thermophilic bacterial periplasmic binding protein to measure branched-chain amino acids and aromatic amino acids

Abstract

Background: The Fischer ratio (ratio between BCAAs and AAAs concentrations) has been considered as an indicator of hepatic disease involving metabolic dysfunctions since its instigation in the 1970's. These amino acids are usually measured by HPLC, gas chromatography and enzymatic spectrophotometry. Considering the future potential of PBPs in clinical diagnosis, LIVBP from a thermophilic bacterium *Thermotoga maritima* was purified and characterized, and evaluated its binding properties with twenty amino acids. The protein's stereo-specificity was also tested due to its importance in astrobiology research. Amino acids and carbohydrates are both known to exist in extraterrestrial environments, and stereo-chemistry is the key aspect for distinguishing between abiotic and biotic origin.

Results: Single amino acid substitutions were generated by overlapping PCR mutagenesis using mutagenic primers to construct two mutants of LIVBP. The first mutant of LIVBP in which Phe at 118 position was replaced with Cys was termed as LIVBP-F118C and the resultant plasmid was named as pKM242. Another mutant of LIVBP in which Asp at 221 position was replaced with Cys was termed as LIVBP-D221C and the resultant plasmid was named as pKM244. Since the LIVBP-F118C showed higher labeling and FRET efficiency compared to that of D221C, the LIVBP-F118C was used for further study.

Conclusion: FRET technology was applied to measure K_d where chimeric LIVBP was engineered to conjugate a donor fluorophore at amino-terminal and an acceptor fluorophore at the incorporated Cys residue. It has been found that LIVBP from *T. maritima* binds with fourteen amino acids out of twenty including branched-chain amino acids (BCAAs) and aromatic amino acids (AAAs) with K_d values ranging from 10^{-6} to 10^{-9} M. The K_d values of BCAAs, AAAs, Met and Cys were observed at nM level. Highest K_d value was observed for L-Leu (37.2 nM) and L-Phe (44.6 nM). These results indicate that $LIVBP_{T.\ maritima}$ has a broader substrate specificity than previously reported for LIVBP proteins from other organisms, which might help for the development of a miniaturized and noninvasive biosensor to measure BCAAs and AAAs.

Keywords: FRET, *Thermotoga maritima*, biosensor, Fischer ratio, branched-chain amino acids, aromatic amino acids, periplasmic binding proteins.

Background

Periplasmic binding proteins (PBPs) are a superfamily of proteins in gram-negative bacteria, responsible for essential nutrients uptake and active transport of biochemical substances such as carbohydrates, amino acids, anions, metal ions and peptides [1, 2, 12]. Previous biological and biochemical studies have shown that these PBPs share some common properties although their size and amino acid sequences may be quite different [3]. In general, PBPs are monomeric and consist of two globular lobes surrounding a ligand binding site where the two lobes are connected by a flexible hinge. PBPs exhibit drastic conformational changes upon ligand binding in which a hinge-twist motion brings the two lobes close together and these mechanism has led the researchers to design several biosensing systems for industry, biology and medicine as well as for astrobiology research [4-7].

Ligand specificity of PBPs is one of the advantageous properties. However, their specificities are strongly dependent on the nature and role of the transport system in the original microorganisms, where they are usually involved in group-specific transport systems. For example, Leucine/Isoleucine/Valine-binding protein (LIVBP) is a component of the branched chain amino acids (BCAAs) group-specific transport system in *Escherichia coli* [8]. Binding studies showed that LIVBP from *E. coli* binds with the BCAAs Leu with K_d value of 2.3×10^{-6} M, Ile with K_d value of 0.9×10^{-6} M and Val with K_d value of 4.0×10^{-6} M [9]. Research works have also reported that LIVBP acts as the third phenylalanine transporter in *E. coli* [10, 11] and might have a broader substrate specificity.

Recently, a fluorescence sensing system for the measurement of BCAAs has been reported based on engineered LIVBP conjugated with environmentally sensitive fluorescence probes [7]. Free amino acids in plasma particularly the BCAAs L-Leu, L-Ile and L-Val as well as aromatic amino acids (AAAs) and methionine are frequently measured to diagnose the patients with hepatic disorders and metabolic abnormalities [13]. The Fischer ratio (ratio of BCAAs concentration to AAAs concentration) has been considered as an indicator of hepatic disease involving metabolic dysfunctions since its instigation in the 1970's [14, 15]. Until today, these amino acids are usually determined by HPLC, gas chromatography and enzymatic spectrophotometry [16, 17]. Considering the future potential of PBPs in clinical diagnosis, we hereby purified and characterized LIVBP from a thermophilic bacterium *Thermotoga maritima*, and evaluated its binding capabilities with twenty amino acids. The protein's stereo-specificity was also tested due to its importance to the astrobiology research. Amino acids and carbohydrates are both known to exist in extraterrestrial environments, and stereo-chemistry is the key aspect for distinguishing between abiotic and biotic origin.

In this research works, we have explored the possibility to develop a fluorescence resonance energy transfer (FRET) based novel biosensing system from thermophilic bacteria since thermal stability of PBPs would provide an advantage for potential future use in a device setting. FRET is a nonradiative, dipole-dipole coupling process where energy from an excited donor fluorophore is transferred to an acceptor fluorophore in close proximity (typically within 10 nm), which makes this method well suited for studying many biological systems [18]. FRET based sensors by fusing a pair of fluorescent proteins to various sites within maltose, ribose, glutamate and phosphate binding proteins have been reported [19-21]. These

fusion exhibited good signal-to-noise ratios and could be directly expressed in bacteria or eukaryotes to study the flux of small molecules within cytoplasm or on the cell surface. However, they are limited to the existing fluorescent proteins for their fluorophore components, and allosteric linkage between ligand binding and chromophore rearrangement [5]. In addition, fusion-based FRET technologies are also limited by linker truncation or by insertion of chromophores into the binding protein at rationally designed sites in order get tighter allosteric linkage between PBP and chromophores. In this research, we therefore explored the attachment of commercially available small-molecule fluorophores into PBPs to occur FRET, which allow the tuning of optical properties with a wider range of absorbance and emission spectra, larger stokes shifts and more resistance to photobleaching.

Materials and Methods

Mutagenesis of LIVBP

PCR was used to amplify the native Leucine-Isoleucine-Valine binding protein (LIVBP) encoding gene *livJ* (TM1135) from genomic DNA of *Thermotoga maritima* strain MSB8. Amplified products were then cloned into an expression vector pAED4 between *NdeI* and *Acc65I* restriction sites. N-terminal oligonucleotide primer was designed to clone the processed periplasmic gene only excluding the signal sequence. The C-terminal primer was designed to append the sequence Gly-Ser-Gly-$(His)_6$ such that the expressed protein would contain the purification handle at its C-terminus [22]. Two tandem stop codons (TAATGA) followed the last $(His)_6$ codon. Single amino acid substitutions were generated by overlapping PCR mutagenesis using mutagenic primers to construct two mutants of LIVBP. *E. coli* strain XL1-BLUE (Stratagene, USA) was used for plasmid constructions. The first mutant of LIVBP in which Phe at 118 position was replaced with Cys was termed as LIVBP-F118C and the resultant plasmid was named as pKM242. Another mutant of LIVBP in which Asp at 221 position was replaced with Cys was termed as LIVBP-D221C and the resultant plasmid was named as pKM244. All clones and mutations were confirmed by DNA sequencing.

Engineered protein expression and purification

The plasmids pKM242 and pKM244 were transformed into BL21-(DE3)-RIL cells (Stratagene, USA), and the proteins without the N-terminal leader sequence (which would direct trafficking to the periplasm) were overexpressed under the control of a strong inducible promoter [22]. A single colony of transformed cells was picked from the agar plate and transferred to 5.0 mL of LB media, both containing ampicillin at 100 µg/mL and chloramphenicol at 34 µg/mL. The culture was grown to saturation (~12 hours), then diluted 1:100 in fresh LB media containing both antibiotics. Cells were grown at 37ºC to an optical density of A_{600} between 0.4 and 0.6. Protein expression was then induced by the addition of 1.0 mM IPTG and continued to grow for 4 hours at 37ºC. Cells were harvested by centrifugation and the pellet was suspended in Buffer-A (10 mM sodium phosphate, 100 mM NaCl, pH 7.5), and stored at -80ºC until purification.

For purification, the cell pellet in Buffer-A was thawed at room temperature. The cells were then sonicated thrice on ice two minutes burst followed by five minutes break) and

centrifuged at 12000 rpm for 20 minutes at 4ºC. Nucleic acids were precipitated from the supernatant by the addition of 2.5% (v/v) of 10% polyamine-P and pelleted by centrifugation at 4ºC. The clear supernatant was loaded onto a Ni-NTA agarose column (Qiagen, USA) which was pre-equilibrated with the Buffer-A. Computer assisted BioLogicLP (Bio-Rad, USA) coupled with automated fraction collector (Bio-Rad, Model 2110, USA) system was used for affinity chromatographic purification of proteins. The $(His)_6$-tagged proteins were eluted using Buffer-B (10 mM sodium phosphate, 100 mM NaCl, 250 mM imidazole, pH 7.5). After purification, the protein was concentrated using a spin concentrator (Centriprep YM-30, Millipore, USA) and concentration was determined by Bradford Assay (Bio-Rad, USA). Bound ligands and salts were removed from LIVBPs by passage through a desalting column (Econo-pac® 10DG, Bio-Rad, USA) using Buffer-C (25 mM sodium phosphate, pH 6.5).

SDS-PAGE analysis of purified proteins

SDS-PAGE was performed on an apparatus (Mini-Protein, Bio-Rad, USA). All protein samples in protein loading buffer (50 mM Tris-Cl, 0.20% sodium dodecyl sulphate, 5.0% glycerol, 80 mM dithiothreitol, 0.0002% bromophenol blue) were heated before loading on the gel for analysis. For fluorescently-labeled samples, gels were imaged by illumination with 305 nm light before staining. All gels were stained with Coomassie Blue R250 and apparent molecular weight were calculated by comparison against commercially available protein marker.

Thiol modification of engineered LIVBP

Purified and concentrated LIVBPs in Buffer-C was diluted in Buffer-D (25 mM sodium phosphate, 1.0 mM tris-2-carboxyethyl-phosphine, pH 7.0) to a concentration of 40 µM. Tetramethyl rhodamine-5-maleimide (TAMRA) (Invitrogen, USA) at a concentration of 800 µM was then added to the protein solution and the reaction was performed according to the manufacturer's protocol. Unbound TAMRA dye was removed from the protein solution by passage through a desalting column (Econo-pac® 10DG, Bio-Rad, USA) using Buffer-C and the resultant TAMRA bound LIVBP was collected, and concentrated using a spin concentrator (Centriprep YM-30, Millipore, USA). This method of purification was found to remove the free dye more efficiently and quickly than the traditional dialysis method.

An N-terminal transamination reaction was performed as described [28]. Briefly, unlabeled protein or TAMRA labeled protein at a concentration of 40 µM was incubated overnight at 65ºC in Buffer-E (25 mM sodium phosphate, 20 mM pyridoxal-5′-phosphate, pH 6.5). Unbound pyridoxal-5′-phosphate (PLP) was removed using a desalting column as described above. The protein containing an N-terminal ketone was then incubated in Buffer-C with 800 µM Alexa-Fluor-488 hydroxylamine (AF488) (Invitrogen, USA). The oxime formation reaction was run overnight at 65ºC and the LIVBPs labeled with AF488 or labeled with both TAMRA and AF488 was again purified using the desalting column as described above.

Determination of fluorophore labeling stoichiometry

The protein concentration of samples was estimated by Bradford assay (Bio-Rad, USA) using BSA as a standard. The concentration of each dye was estimated by its absorbance at λ_{max}.

The extinction coefficient (ε_c) of 70,000 $M^{-1}cm^{-1}$ at 495 nm for AF488 and the ε_c of 65,000 $M^{-1}cm^{-1}$ at 555 nm for TAMRA were used in the calculation. Because the absorbance of one dye will increase the overall absorbance at λ_{max} of the other, the singly labeled conjugates of each dye were also analyzed in this manner. The percent conversion of each reaction was then determined by dividing the dye concentration by the protein concentration.

Fluorescence spectroscopy for ligand binding assay

Spectrofluorometer (FluoroMax-2, Horiba, Japan) was used to acquire the fluorescence excitation and emission spectra. Excitation spectra were recorded by scanning excitation wavelengths from 400 nm to 560 nm, monitoring the emission maximum of the acceptor dye at 570 nm. Emission spectra were recorded from 500 nm to 600 nm, with an excitation wavelength of 470 nm. For ligand binding experiments, emission spectra of the labeled protein at the concentration of 50 nM without ligand in a cuvette containing 1.5 mL Buffer-A were recorded at a specific time interval and evaluated the equilibration state. Once the protein solution was equilibrated, titration experiment was started where the ligand concentration ranged from $1.0x10^{-2}$ M to $1.0x10^{-12}$ M. No significant photobleaching of either dye was observed under the conditions used. Fraction saturation and dissociation constant (K_d) from the best-fit binding curve were calculated as described [4].

Results

Engineering of Leucine-Isoleucine-Valine binding proteins (LIVBPs)

Figure-1A and Figure-1B represent the open form (PDB ID: 1Z15) and the closed form (PDB ID: 1Z16) of LIVBP from *E. coli*, respectively. Since LIVBP from *T. maritima* has not been well studied, crystal structures of both open and closed forms are unknown. Therefore, homology modeling approach was applied to predict the 3D structure of LIVBP from *T. maritima* in open form (Fig. 2a) using the crystal structure of LIVBP from *E. coli* (PDB ID: 1Z15) as a template in order to understand the physical properties of the target protein. PDB ID 1Z15 was used as the template in the homology modeling because analysis of sequence alignment showed slightly higher homology between LIVBP from *E. coli* and *T. maritima* (28.3% identity and 47.3% similarity) compared to that of LeuBP from *E. coli* (PDB ID: 1USG) and LIVBP from *T. maritima* (25.4% identity and 44.0% similarity). It should be noted that amino acid sequence identity between LeuBP and LIVBP from *E. coli* was about 80% (Fig. 3).

Research works have shown that Ser79, Ala100. Thr102, Tyr202 and Glu226, located at the cleft between the two domains of *E. coli* LIVBP, are responsible for ligand binding [29] (Fig. 1). Based on the homology modeling, their counter parts in *T. maritima* LIVBP were predicted as Ser75, Ala96, Thr98, Tyr197 and Asp221, and these information was used to engineering the candidate sites for fluorophore attachment. One candidate site for fluorophore attachment was chosen at 118 position and substituted that amino acid (Phe) with Cys, and the resultant mutant protein was termed as LIVBP-F118C (Fig 2a). Another site for fluorophore attachment was chosen at 221 position and substituted that amino acid (Asp) with Cys, and the resultant mutant protein was termed as LIVBP-D221C (Fig. 2a). The latter site for fluorophore attachment was chosen to investigate the effect of Cys substitution at

Asp221 because this amino acid has been predicted to be involved in ligand binding based on the simulated 3D structure. Since the LIVBP encoded gene from *T. maritima* had a Cys residue at 113 position (Fig. 3), the native Cys was replaced with Ala (C113A) in order to eliminate cross-reaction between fluorophores and the resultant plasmid was used to create site-specification point mutation as mentioned in the method section.

Fluorophore labeling and characterization of engineered LIVBPs

Tetramethyl rhodamine-5-maleimide (TAMRA) was conjugated to LIVBP-F118C based on the cysteine chemistry with 45% efficiency whereas conjugation of Alexa-Fluor-488 hydroxylamine (AF488) to the N-terminal end of LIVBP-F118C yielded 38% efficiency (Fig. 4a). On the other hand, 9% conversion in TAMRA reaction and 40% conversion in the two-step transamination/oxime formation reactions were achieved for LIVBP-D221C (Fig. 4b). Percent conversions were estimated by the Bradford/UV-Vis method as described in method section. Extinction coefficients for each conjugated dye were obtained from the supplier and differed from the values for free dye (Molecular Probes "Amine-Reactive Handout"). The order of labeling reactions did not affect the final percentage of conversions. It was found that LIVBP-D221 was poorly labeled with TAMRA (Fig. 4b).

These results showed that LIVBP-F118C exhibited observable FRET (Fig. 5a). Non-radiative energy was transferred from donor to acceptor as was observed as quenching of AF488 emission in the doubly-labeled protein conjugate. Another mutant protein LIVBP-D221C did not show quenching of AF488 emission in the doubly-labeled protein conjugate and thus no observable FRET (Fig. 5b). Ligand dependent conformational changes in FRET efficiency were initially investigated for both labeled LIVBP-F118C and LIVBP-D221C using L-Ile as ligand. Upon ligand binding, LIVBP-F118C underwent conformational change that brought the dyes close together and thus affected the efficiency of energy transfer (Fig. 6). On the other hand, labeled LIVBP-D221C did not exhibit any change upon ligand binding. Therefore, LIVBP-F118C was considered as a potential sensor and thus investigated further to explore its ligand binding characteristics.

Binding study of LIVBP-F118C with branched-chain amino acids (BCAAs)

Binding study of LIVBP-F118C with BCAAs, which was conjugated with a pair of fluorescence probes to achieve observable FRET, showed the K_d of 37.2 nM for L-Leu, 153.6 nM for L-Ile and 217.9 nM for L-Val (Fig. 7). In order to check the stereo-specificity, labeled LIVBP-F118C was titrated against D-Leu, D-Ile and D-Val. It was found that the FRET-based LIVBP-F118C sensor was very specific for L-isomers except for D-Leu. The K_d of 94.3 μM for D-Leu was calculated from the best-fit binding curve (Fig. 8). Since affinity for D-Leu was appeared to be very unusual, possible trace contamination of L-Leu in the supplied D-Leu was suspected. Therefore, labeled LIVBP-F118C was tested with D-Leu obtained from another manufacturer and the K_d of 8.42 μM was obtained (Fig. 9). Due to the significant K_d differences between two manufacturer's D-Leu, it was reasonable to conclude that none of these D-Leu was pure. In order to test the effect of trace contamination, labeled LIVBP-F118C was titrated with DL-Ile (50% L-Ile and 50% D-Ile) and the K_d of 373.3 nM was calculated (Fig. 9), which was very comparable to that of pure L-Ile (Fig. 7). Although we did not test the labeled LIVBP-F118C with D-Leu from 3rd manufacturer, it was reasonable to

speculate that binding affinity of LIVBP-F118C for D-Leu was due to the trace contamination of L-Leu because the experimental results with DL-Ile clearly indicated a profound effect on binding affinity due to trace contamination.

Binding study of LIVBP-F118C with aromatic amino acids (AAAs)

Binding studies of LIVBP-F118C revealed that LIVBP from *T. maritima* strongly binds with AAAs, especially with L-Phe. The calculated K_d for L-Phe, L-Tyr and L-Trp obtained from best-fit binding curve was 44.6 nM, 177.9 nM and 274.4 nM, respectively (Fig. 10). This FRET-based LIVBP sensor was also titrated with D-Phe, D-Tyr and D-Trp in order to check its stereo-specificity. The results showed that none of these D-isomers bound with LIVBP. The binding affinity of LIVBP-F118C for L-Phe (Fig. 10) was almost similar to that of L-Leu (Fig. 7).

Titration of LIVBP-F118C with other amino acids

Titration of labeled LIVBP-F118C with L-Ser and L-Thr exhibited that the binding affinity for L-Ser was much lower than that of L-Thr. The calculated K_d for L-Ser was 19.7 μM and 1.03 μM for L-Thr (Fig 11). Binding study of LIVBP-F118C with L-Cys, L-Asn and L-Gln was also performed. The calculated K_d was 213.2 nM for L-Cys, 2.81 μM for L-Asn and 6.58 μM for L-Gln (Fig. 12), indicating that LIVBP has a broader substrate specificity than previously reported. The binding affinity for L-Cys was very comparable to that of L-Ile, L-Val, L-Met, L-Tyr and L-Trp. Moreover, titration of FRET-based LIVBP sensor with L-Ala, L-Met and L-Glu has been performed (Fig. 13). As was observed from the experiments, the calculated K_d was 4.59 μM for L-Ala, 11.49 μM for L-Glu and 254.8 nM for L-Met. Titration of LIVBP-F118C with acidic (Asp and Glu) and basic (Arg, His and Lys) polar AAs revealed that none of these ligands bind with LIVBP except L-Glu. Furthermore, the FRET-based LIVBP sensor from the thermophilic bacterium *T. maritima* was titrated with L-Gly and L-Pro, and the results showed that any of these ligands did not bind with LIVBP-F118C.

Discussion

Research on biosensors has greatly increased in recent years because of biosensors' widespread potential applications and remarkable ability to measure the presence of a single molecular species in a complex mixture. However, before invention of protein-engineering techniques, the only available biomolecules to construct biosensors were naturally occurring macromolecule with proper signal transduction mechanism and the desired analyte specificity from a number of candidates, and then device a detector to adapt to that mechanism [23]. Although a number of biosensors have been developed in this manner, this method is case-specific and laborious. With the advancement of protein-engineering techniques, the number of strategies for developing biosensors has been greatly increased. We can now develop biosensors not only in the way described above, but also by incorporating reporter groups such as fluorophores directly into biological molecules with desired analyte specificity, thus making them suitable to the available detectors [24, 4]. In this study, genetic engineering techniques were applied to manipulate the LIVBP from thermophilic *T. maritima* in order to explore its potential to the sensing applications.

As shown in Fig. 4b, LIVBP-D221 was poorly labeled with TAMRA. Lower labeling

efficiency of LIVBP-D221C with TAMRA was not surprising because simulated 3D structure of the protein revealed that thiol-reactive group of Cys residue was found to be poorly exposed to the aqueous surface compared to those of LIVBP-F118C (Fig. 2b). Fluorescence emission spectra of LIVBP-F118C and LIVBP-D221C labeled with single AF488 dye or both AF488 and TAMRA dyes were taken, and normalized fluorescence intensity was plotted against wavelength (Fig. 5). It was found that the LIVBP-D221C did not show quenching of AF488 emission in the doubly-labeled protein conjugate and thus no observable FRET was observed (Fig. 5b). The reason was probably due to poorly labeling of LIVBP-D221 with TAMRA or the distance between donor and acceptor was not favorable to occur FRET. As shown in Fig. 6, the FRET efficiency of LIVBP-F118C was reduced after ligand binding. The reason was due to the fact that the rate of energy transfer also depends on the relative orientations of transition dipole moments of the donor and acceptor.

Branched-chain amino acids (BCAAs) refer to the amino acids having aliphatic side-chains that are non-linear. The combination of these BCAAs (Leu, Ile and Val) makes up approximately one-third of skeletal muscle in human, and plays an important role in protein synthesis and insulin metabolism [25, 26]. Therefore, the sensors with high sensitivity and group-specific molecular recognition ability would be very much desirable for medical communities and also for astrobiology researches in order to detect *in situ* biogenic molecules in the extraterrestrial environments. Chino and coworkers [7] reported a fluorescence sensing system for BCAAs based on engineered LIVBP from *E. coli* conjugated with environmentally sensitive fluorescence probes, and the binding study with ligands reported the K_d of 0.5 μM for Leu, 0.2 μM for Ile and 1.1 μM for Val. These results were somewhat similar with those reported previously for the native LIVBP from *E. coli* (K_d of 2.3 μM for Leu, 0.9 μM for Ile and 4.0 μM for Val) [9]. The engineered LIVBP from *T. maritima* conjugated with a pair of fluorescence probes to achieve observable FRET showed the K_d of 37.2 nM for L-Leu, 153.6 nM for L-Ile and 217.9 nM for L-Val (Fig. 7). It should be noted that FRET based LIVBP-F118C exhibited very strong affinity for non-β-branch of BCAA (Leu) compared to that of β-branch of BCAAs (Ile and Val). The reason was probably due to the presence of a methyl group ($-CH_3$) located at the β-carbon, which seemed to be less favorable to the binding pocket of LIVBP. Binding study of LIVBP-F118C with D-Leu, D-Ile and D-Val revealed that this FRET-based sensor was very specific for L-isomers except for D-Leu (Fig. 8). The reason might be due to the trace contamination of L-Leu because the experimental results with DL-Ile (Fig. 9) clearly indicated a profound effect on binding affinity due to trace contamination.

Aromatic amino acids (AAAs) includes Phe, Tyr and Trp, and among them Phe is hydrophobic while other two are slightly hydrophilic. Chino and coworkers [7] showed that LIVBP from *E. coli* had no binding affinity for AAAs. Previous research works have showed that leucine binding protein (LeuBP), which has about 80% amino acid sequence identity with LIVBP, bound Phe with K_d of 180 nM whereas LIVBP did not bind with Phe [29]. However, other research works have showed that the LIVBP/LBP system (also known as BCAA transporter) acted as the third Phe transporter and played a significant role in the accumulation of Phe in the growth of Phe-auxotrophic *E. coli* strains [11]. It was found that the binding affinity of LIVBP-F118C for L-Phe (Fig. 10) was almost similar to that of L-Leu

(Fig. 7). The reason was probably due to fact that both Phe and Leu are hydrophobic in nature and share structural similarity except aromatic ring. These experimental results suggest that branched or complexed aromatic ring are not so favorable to the binding pocket of LIVBP from *T. maritima* as was observed for L-Phe but their molecular mechanisms have not been yet understood clearly.

Research works have showed that LIVBP from *E. coli* also binds with Ser, Thr and Ala although their binding affinities are much lower compared to that of Ile, Leu and Val [11, 27]. These results suggested that LIVBP might have broader substrate specificity than expected since no further experiments have been reported so far. Therefore, the FRET-based LIVBP sensor was further tested with rest of the other amino acids in order to explore its binding capabilities. Binding studies of LIVBP-F118C with L-Ser and L-Thr exhibited that the binding affinity for L-Ser was much lower than that of L-Thr (Fig 11). These results suggest that like *E. coli*, entry of L-Ser and L-Thr into *T. maritima* appears to be mediated also by the LIVBP system. As shown in Fig. 13, binding affinity of LIBVP-F118C for L-Ala was not surprising because previous research works reported that L-Ala binds with LIVBP from *E. coli* [11, 27], indicating that entry of L-Ala in both organisms is also mediated by LIVBP system.

Conclusion

We reported here the construction of a novel fluorescence sensing system using FRET-based technology. LIVBP from *T. maritima* was engineered to conjugate the donor fluorophore AF488 at N-terminal of the protein and the acceptor fluorophore TAMRA at the incorporated cysteine residue in order to occur FRET. The developed FRET-based LIVBP sensor was then titrated with twenty amino acids and the K_d values were calculated from the best-fit binding curves. The experimental results have showed that LIVBP from *T. maritima* binds with fourteen amino acids out of twenty with K_d values of 10^{-6} to 10^{-9} M. The experimental results have showed that LIVBP from *T. maritima* strongly bound with L-Leu (K_d of 37.2 nM) and L-Phe (K_d of 44.6 nM) as well as moderately binds with L-Ile (K_d of 153.6 nM), L-Val (K_d of 217.9 nM), L-Met (K_d of 254.8 nM), L-Tyr (K_d of 177.9 nM), L-Trp (K_d of 274.4 nM) and L-Cys (K_d of 213.2 nM). LIVBP from *T. maritima* also poorly bound with L-Ser (K_d of 19.7 μM), L-Thr (K_d of 1.03 μM), L-Asn (K_d of 2.81 μM), L-Gln (K_d of 6.58 μM), L-Ala (K_d of 4.59 μM) and L-Glu (K_d of 11.49 μM). It should be noted that the FRET-based LIVBP sensor was very specific for L-isomers, which make this new sensing system ideally suitable for astrobiology research. In addition, the specific sensitivity and group-specific molecular recognition ability of our FRET-based LIVBP sensor also make this system ideally suited to measure the concentrations of medically important BCAAs and AAAs as well as Met from the blood plasma for diagnosing the metabolic abnormalities and hepatic disorders.

References

1. Haiso CD, Sun YJ, Rose J, Wang BC (1996) The crystal structure of glutamine binding protein from *Escherichia coli*. J. Mol. Biol. 262:225-242.
2. Sun YJ, Rose J, Wang BC, Haiso CD (1998) The structure of glutamine binding protein

complexed with glutamine at 1.94A resolution: Comparison with other amino acid binding proteins. J. Mol. Biol. 278:219-229.
3. Quiocho FA (1990) Atomic structure of periplasmic binding proteins and the high-affinity active transport systems in bacteria. Phil. Trans. Roy. Soc. B Biol. Sci. 326:341-351.
4. de Lorimer RM, Smith JJ, Dwyer MA, Looger LL, Sali KM, Paavola CD, Rizk SS, Sadigov S, Conrad DW, Loew L, Hellinga HW (2002) Construction of a fluorescent biosensor family. Prot. Sci. 11:2655-2675.
5. Deuschle K, Okumoto S, Fehr M, Looger LL, Kozhukh L, Frommer WB (2005) Construction and optimization of a family of genetically encoded metabolite sensors by semirational protein engineering. Prot. Sci. 14:2304-2314.
6. Dwyer MA, Hellinga HW (2004) Periplasmic binding proteins: a versatile superfamily for protein engineering. Cyrr. Opin. Struc. Biol. 14:495-504.
7. Chino S, Sakaguchi A, Yamoto R, Ferri S, Sode K (2007) Branched-chain amino acid biosensing using fluorescent modified engineered leucine/isoleucine/valine binding protein. Int. J. Mol. Sci. 8:513-525.
8. Oxender DL, Anderson JJ, Daniels CJ, Landick R, Gunsalus RP, Zurawski G, Selker E, Yanofsky C (1980) Structural and functional analysis of cloned DNA containing genes responsible for branched-chain amino acid transport in *Escherichia coli*. Proc. Natl. Acad. Sci. USA. 77:1412-1416.
9. Vorotyntseva TI, Surin AM, Trakhanov SD, Nabiev IR, Antonov VK (1981) Spectral properties of the leucine-isoleucine-valine binding protein and its complexes with substrates. Bioorg. Khim. 7:45-57.
10. Landick R, Oxender DL (1985) The complete nucleotide sequences of the *Escherichia coli* LIV-BP and LS-BP genes. Implication for the mechanism of high-affinity branched-chain amino acid transport. J. Biol. Chem. 260:8257-8261.
11. Koyanagi T, Katayama T, Suzuki H, Kumagai H (2004) Identification of the LIV-I/LS system as the third phenylalanine transporter in *Escherichia coli* K-12. J. Bacteriol. 186:343-350.
12. Ames GFL (1986) Bacterial periplasmic transport systems: Structure, mechanism and evolution. Annu. Rev. Biochem. 55:397-425.
13. Fischer JE, Rosen HM, Ebeid AM, James JH, Keane JM, Soeters PB (1976) The effect of normalization of plasma amino acids on hepatic encephalopathy in man. Surgery 80:77-91.
14. Nishitani S, Ijichi C, Takehana K, Fujitani S, Sonaka I (2004) Pharmacological activities of branched-chain amino acids: specificity of tissue and signal transduction. Biochem. Biophys. Res. Commun. 313:387-389.
15. Nieuwoudt M, Kunnike R, Smuts M, Becker J, Stegmann GF, van der Walt C, Neser J, van der Merwe S (2006) Standardization criteria for an ischemic surgical model of acute hepatic failure in pigs. Biomaterials 27:3836-3845.
16. Hughes GJ, Winterhalter KH, Boller W, Wilson KJ (1982) Amino acid analysis using standard high performance liquid chromatography equipment. J. Chromatogr. 235:417-426.
17. Nanashima A, Yamaguchi H, Shibasaki S, Abo T, Morino S, Yoshinaga M, Sawai T,

Tanaka K, Hidaka S, Tsuji T, Nakagoe T, Ayabe H (2003) Changes of branched chain amino acids and tyrosine ratio (BTR) after hepatectomy. Acta. Med. Nagasaki 48:29-33.
18. Wu P, Brand L (1994) Resonance Energy Transfer: Methods and Applications. Analytical Biochemistry, 218, 1-13.
19. Fehr M, Okumoto S, Deuschle K, Lager I, Looger LL, Persson J, Kozhukh L, Lalonde S, Fromer WB (2005) Development and use of fluorescent nanosensors for metabolite imaging in living cells. Biochem. Soc. Trans. 33:287-290.
20. Okumoto S, Looger LL, Micheva KD, Reimer RJ, Smith SJ, Frommer WB (2005) Detection of glutamate release from neurons by genetically encoded surface-displayed FRET nanosensors. Proc. Natl. Acad. Sci. USA. 102:8740-8745.
21. Gu H, Lalonde S, Okumoto S, Looger LL, Scharff-Poulsen AM, Grossman AR, Kossmann J, Jakobsen I, Frommer WB (2006) A novel analytical method for *in vivo* phosphate tracking. FEBS Lett. 580:5885-5893.
22. Crochet AP, Kabir MM, Francis MB, Paavola CD (2010) Site-selective dual modification of periplasmic binding proteins for sensing applications. Biosens. Bioelectron. 26:55-61.
23. Hellinga HW, Marvin JS (1998) Protein engineering and the development of generic biosensors. Trends Biotechnol. 16:183-189.
24. Salins LLE, Ware RA, Ensor CM, Daunert S (2001) A novel reagentless sensing system for measureing glucose based on the glucose/galactose binding protein. Anal. Biochem. 294:19-26.
25. Karlsson HK, Nilsson PA, Nilsson J, Chibalin AV, Zierath JR, Blomstrand E (2004) Branched-chain amino acids increase p70S6k phosphorylation in human skeletal muscle after resistance exercise. Am. J. Physiol. Endocrinol. Metab. 287:E1-E7.
26. Blomstrand E, Eliasson J, Karlsson HK, Köhnke R (2006) Branched-chain amino acids activate key enzymes in protein synthesis after physical exercise. J. Nutr. 136:269S–273S.
27. Oxender DL, Quay S (1975) Binding proteins and membrane transporter. Annals NY Acad. Sci. 264:358-372.
28. Gilmore JM, Scheck RA, Esser-Kahn AP, Joshi NS, Francis MB (2006) N-terminal protein modification through a biomimetic transamination reaction. Angew. Chem. Int. Ed. 45:5307-5311.
29. Magnusson U, Salopek-Sondi B, Luck LA, Mowbray SL (2004) X-ray structures of the leucine-binding protein illustrate conformational changes and the basis of ligand specificity. J. Biol. Chem. 279:8747-8752.

Figure legends

Fig. 1: X-ray 3D structure of LIVBP from *E. coli* in open form (PDB ID: 1Z15) (a) and closed form (PDB ID:1Z16) (b). Red sphere in (b) represents the ligand L-Leu bound to the protein.

Fig. 2: Simulated 3D structure of LIVBP from *T. maritima*. The Cys substitution sites (D221, F118 and C113) are marked in magenta color (a), and the thiol-reactive groups of inserted Cys residues are shown in the zoomed section as blue-spheres whereas magenta-spheres represent the other functional groups of Cys (b). The upper and lower spheres in (b) are for 118C and 221C, respectively.

Fig. 3: Alignment of amino acid sequences of LeuBP (PDB ID: 1USG) and LIVBP (PDB ID: 1Z15) from *E. coli* as well as LIVBP from *T. maritima* (TM1135). Numbering begins from the immediate amino acid next to initiation Met of the open reading frame for 1USG excluding its signal sequence. The native Cys residue in TM1135 is shown as bold and underlined.

Fig. 4: Absorbance of LIVBP-F118C (a) and LIVBP-D221C (b) labeled with AF488 (solid line), and both AF488 and TAMRA fluorophore (dotted line). All spectra were normalized to the concentration of AF488.

Fig. 5: Fluorescence emission spectra of LIVBP-F118C (a) and LIVBP-D221C (b) labeled with AF488 fluorophore (solid line), and labeled with both AF488 and TAMRA fluorophore (dotted line). All spectra were normalized to the fluorescence intensity of AF488.

Fig. 6: Fluorescence emission spectra of LIVBP-F118C labeled with both AF488 and TAMRA fluorophore before (solid line) and after addition of the ligand L-Ile at a concentration of 9.9×10^{-5} M (dotted line).

Fig. 7: Fluorimetric titration of engineered LIVBP-F118C with L-Ile (●), L-Leu (o) and L-Val (□). The lines shown are the best-fit binding curves for each ligand.

Fig. 8: Fluorimetric titration of engineered LIVBP-F118C with D-Ile (●), D-Leu (o) and D-Val (□). The lines shown are the best-fit binding curves for each ligand.

Fig. 9: Fluorimetric titration of labeled LIVBP-F118C with DL-Ile (50% L-Ile and 50% D-Ile) (●) and D-Leu (o). An asterisk on D-Leu represents that this batch was obtained from another manufacturer and the lines shown are the best-fit binding curve for the respective ligands.

Fig. 10: Fluorimetric titration of FRET-based LIVBP sensor with L-Tyr (●), L-Trp (o) and L-Phe (□). The lines shown are the best-fit binding curves for each ligand.

Fig. 11: Fluorimetric titration of FRET-based LIVBP sensor with L-Ser (●) and L-Thr (o). The lines shown are the best-fit binding curves for each ligand.

Fig. 12: Fluorimetric titration of FRET-based LIVBP sensor with L-Asn (●), L-Cys (o) and L-Gln (□). The lines shown are the best-fit binding curves for the respective ligands.

Fig. 13: Fluorimetric titration of labeled LIVBP-F118C with L-Ala (●), L-Met (o) and L-Glu (□). The lines shown are the best-fit binding curves for each ligand.

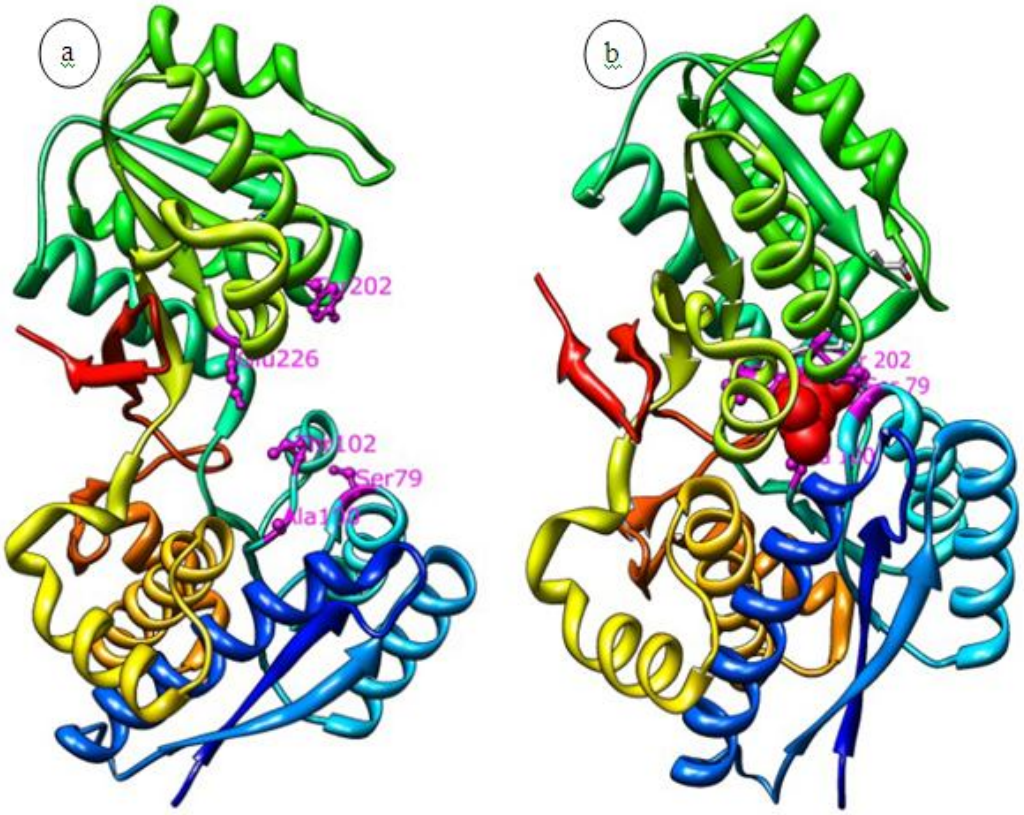

Fig. 1: X-ray 3D structure of LIVBP from *E. coli* in open form (PDB ID: 1Z15) (a) and closed form (PDB ID:1Z16) (b). Red sphere in (b) represents the ligand L-Leu bound to the protein.

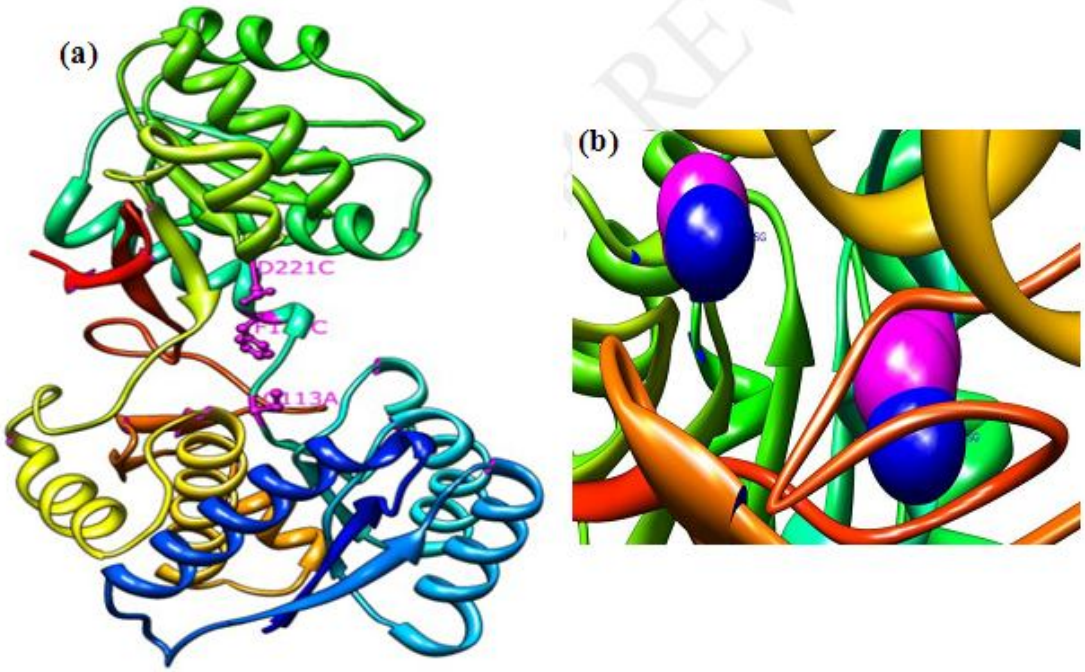

Fig. 2: Simulated 3D structure of LIVBP from *T. maritima*. The Cys substitution sites (D221C, F118C and C113A) are marked in magenta color (a), and the thiol-reactive groups of inserted Cys residues are shown in the zoomed section as blue-spheres whereas magenta-spheres represent the other functional groups of Cys (b). The upper and lower spheres in (b) are for 118C and 221C, respectively.

Fig. 3: Alignment of amino acid sequences of LeuBP (PDB ID: 1USG) and LIVBP (PDB ID: 1Z15) from *E. coli* as well as LIVBP from *T. maritima* (TM1135). Numbering begins from the immediate amino acid next to initiation Met of the open reading frame excluding its signal sequence. The native Cys residue in TM1135 is shown as bold and underlined.

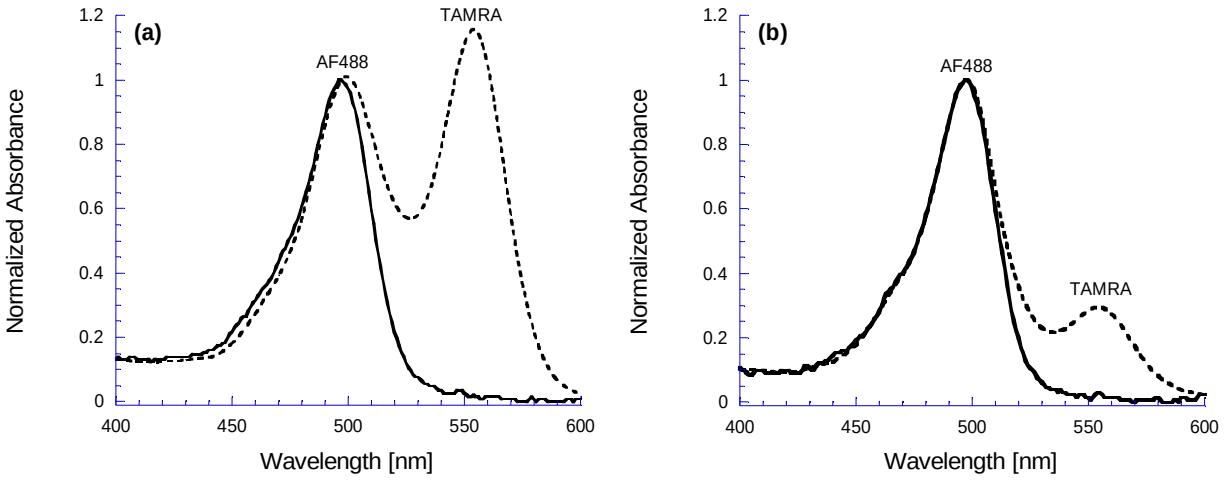

Fig. 4: Absorbance of LIVBP-F118C (a) and LIVBP-D221C (b) labeled with AF488 (solid line), and both AF488 and TAMRA fluorophore (dotted line). All spectra were normalized to the concentration of AF488.

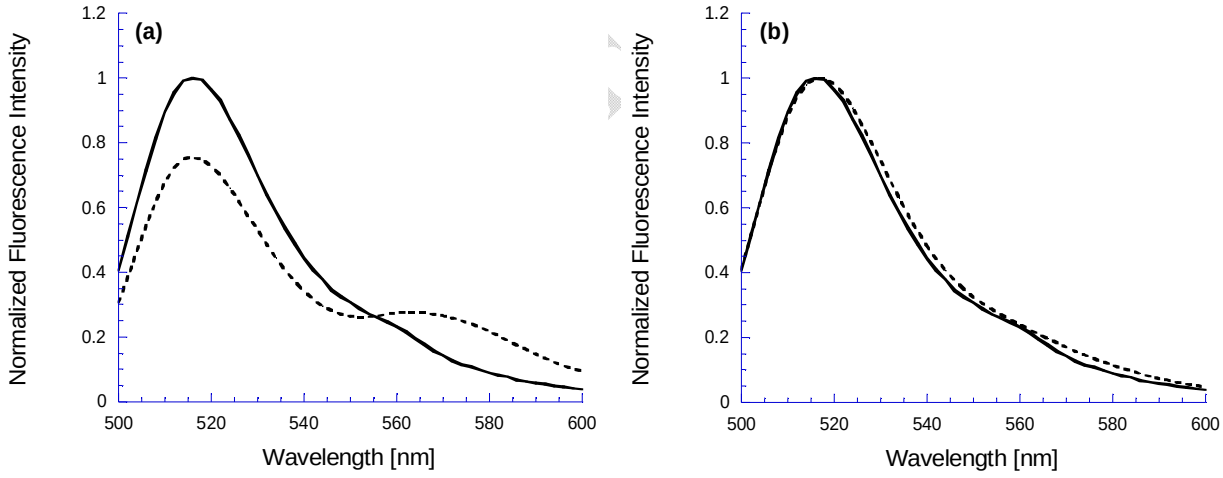

Fig. 5: Fluorescence emission spectra of LIVBP-F118C (a) and LIVBP-D221C (b) labeled with AF488 fluorophore (solid line), and labeled with both AF488 and TAMRA fluorophore (dotted line). All spectra were normalized to the fluorescence intensity of AF488.

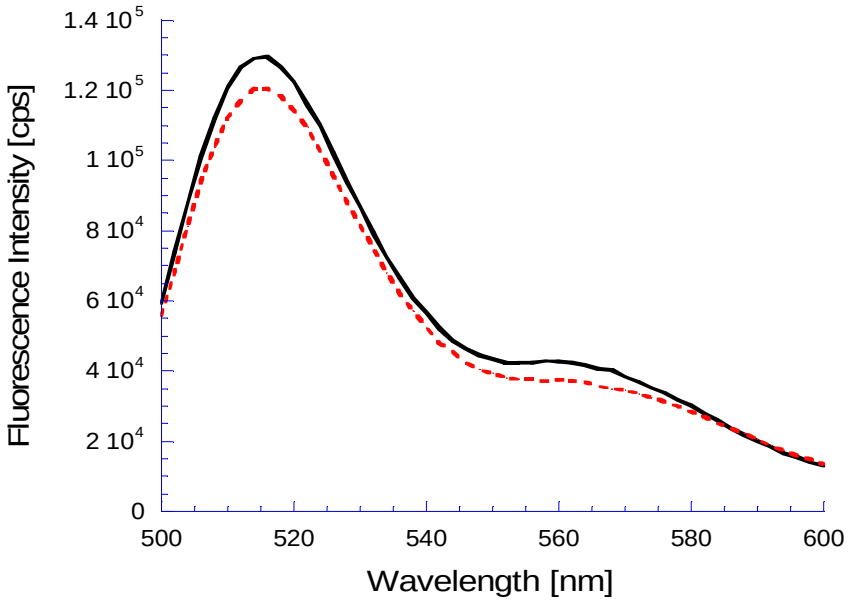

Fig. 6: Fluorescence emission spectra of LIVBP-F118C labeled with both AF488 and TAMRA fluorophore before (solid line) and after addition of the ligand L-Ile at a concentration of 9.9×10^{-5} M (dotted line).

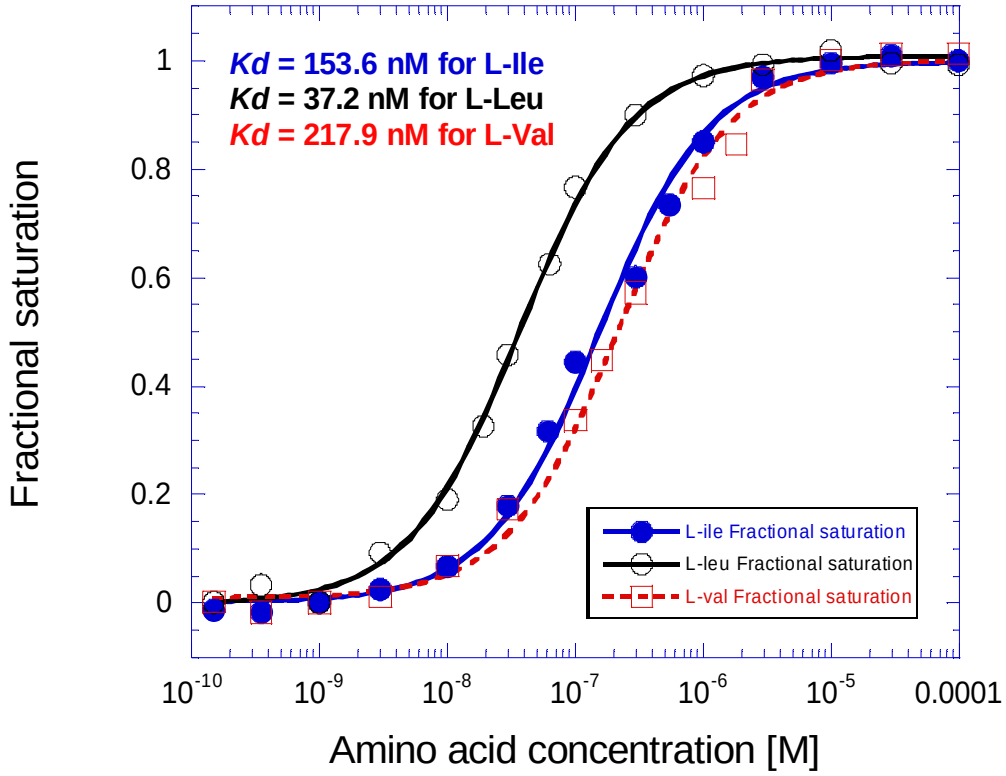

Fig. 7. Fluorimetric titration of engineered LIVBP-F118C with L-Ile (●), L-Leu (o) and L-Val (□). The lines shown are the best-fit binding curves for each ligand.

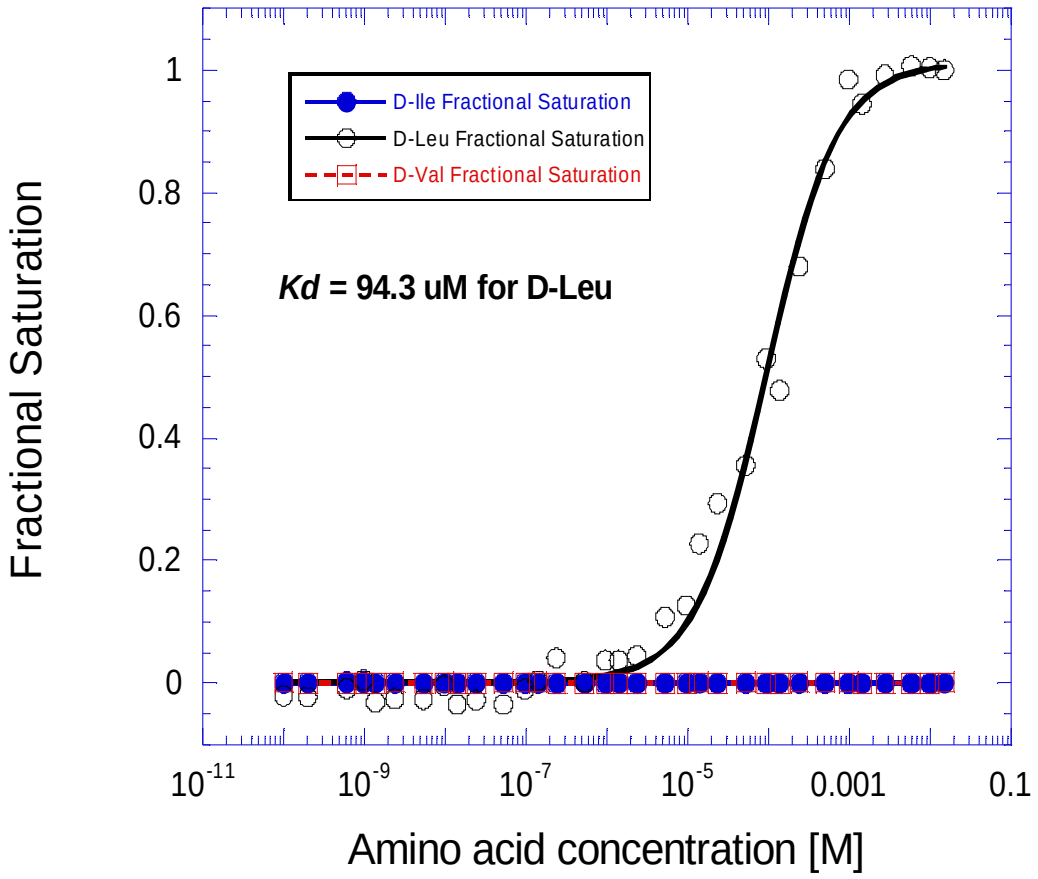

Fig. 8. Fluorimetric titration of engineered LIVBP-F118C with D-Ile (●), D-Leu (o) and D-Val (□). The lines shown are the best-fit binding curves for each ligand.

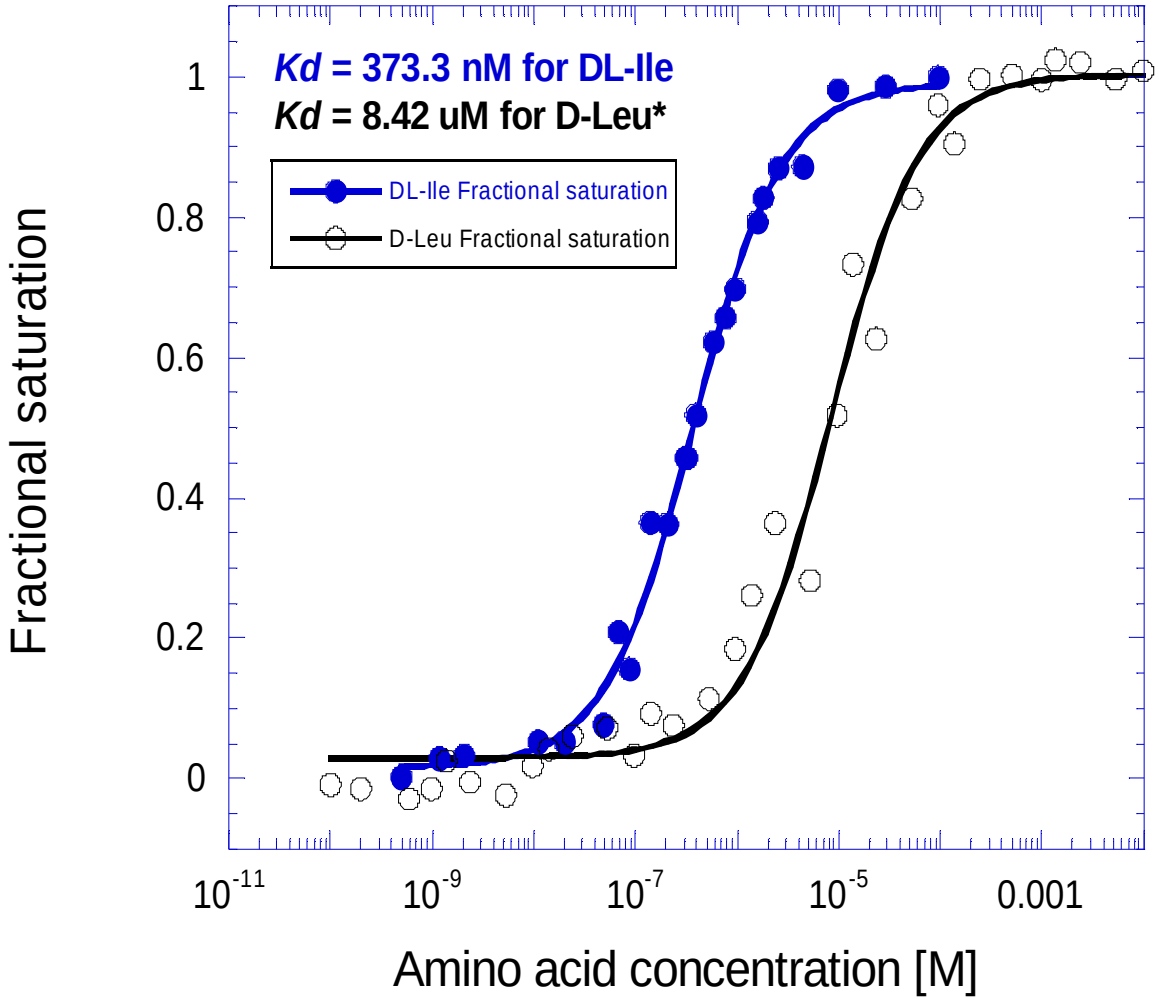

Fig. 9. Fluorimetric titration of labeled LIVBP-F118C with DL-Ile (50% L-Ile and 50% D-Ile) (●) and D-Leu (o). An asterisk on D-Leu represents that this batch was obtained from another manufacturer and the lines shown are the best-fit binding curve for the respective ligands.

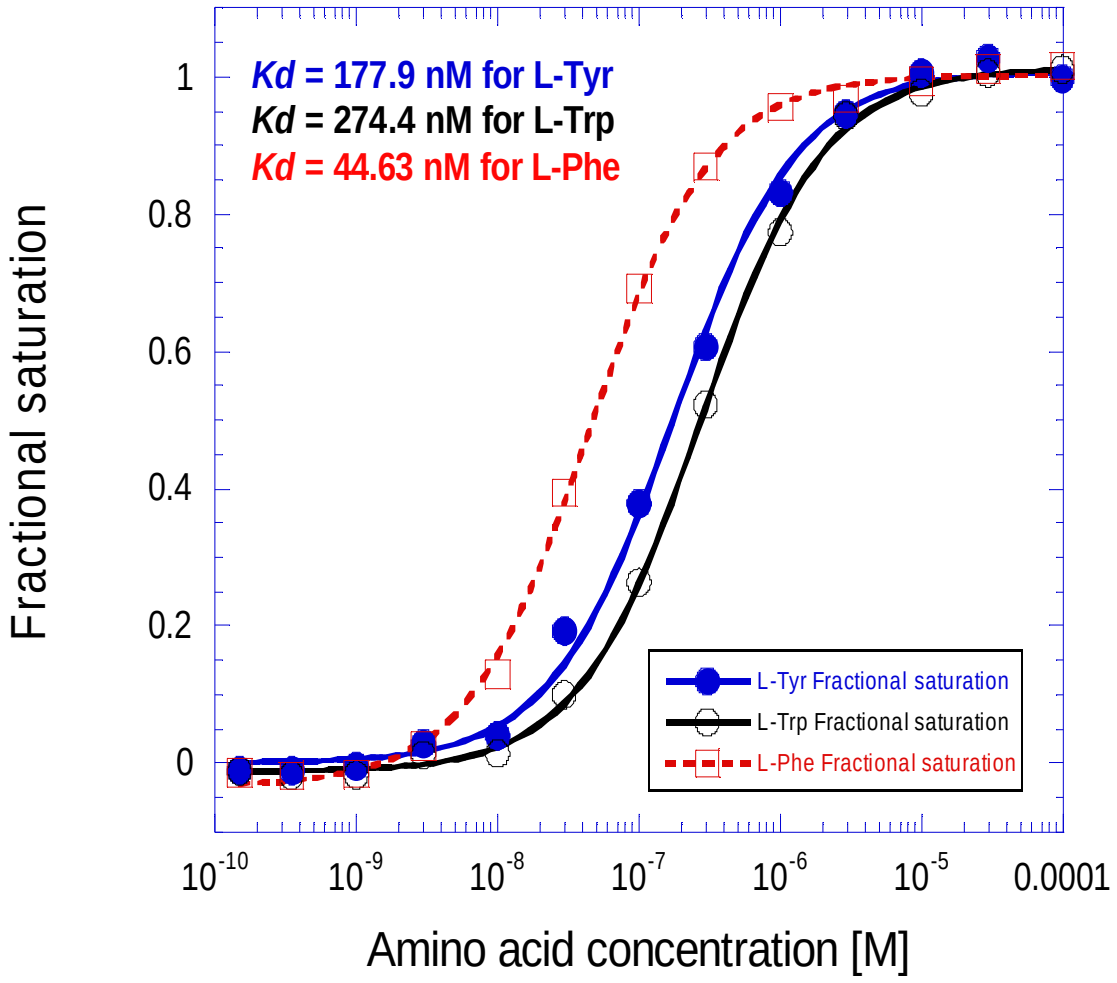

Fig. 10. Fluorimetric titration of FRET-based LIVBP sensor with L-Tyr (●), L-Trp (o) and L-Phe (□). The lines shown are the best-fit binding curves for each ligand.

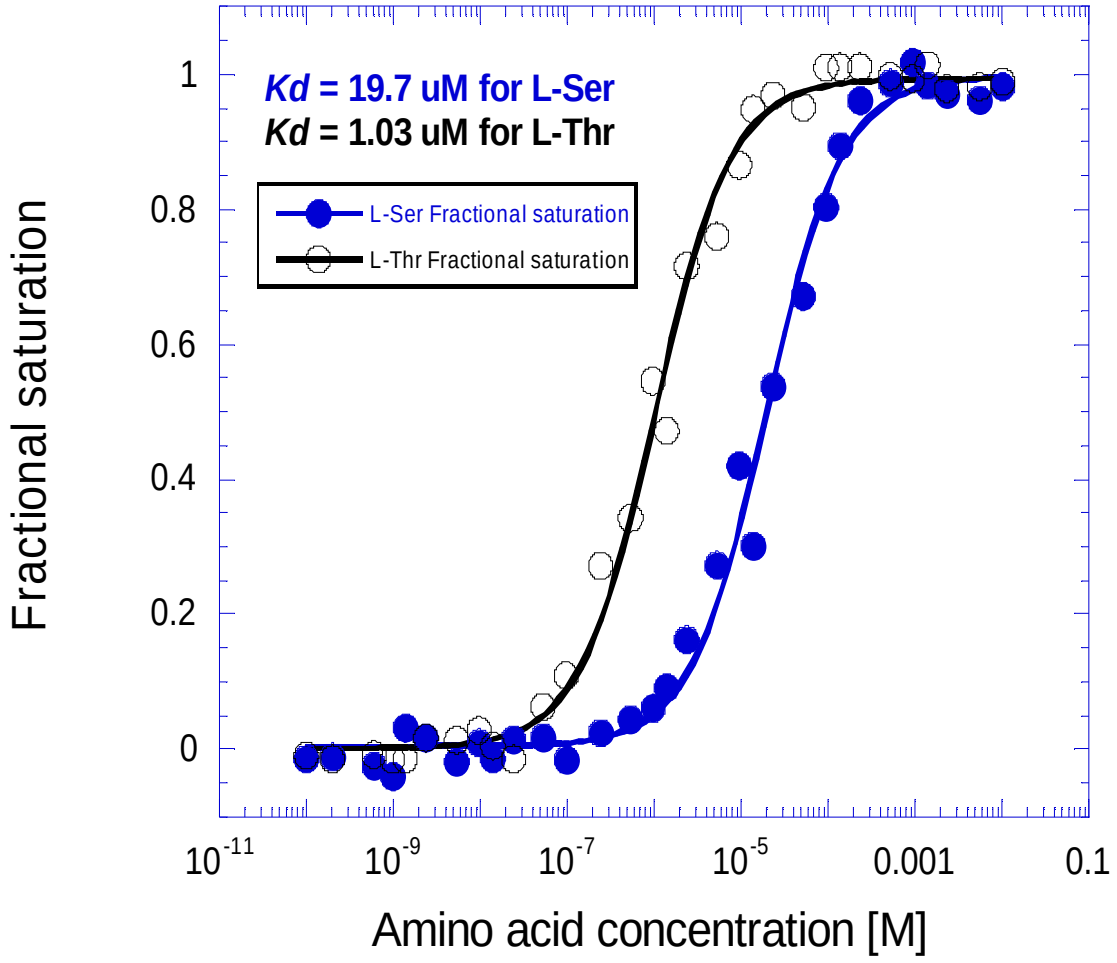

Fig. 11. Fluorimetric titration of FRET-based LIVBP sensor with L-Ser (●) and L-Thr (o). The lines shown are the best-fit binding curves for each ligand.

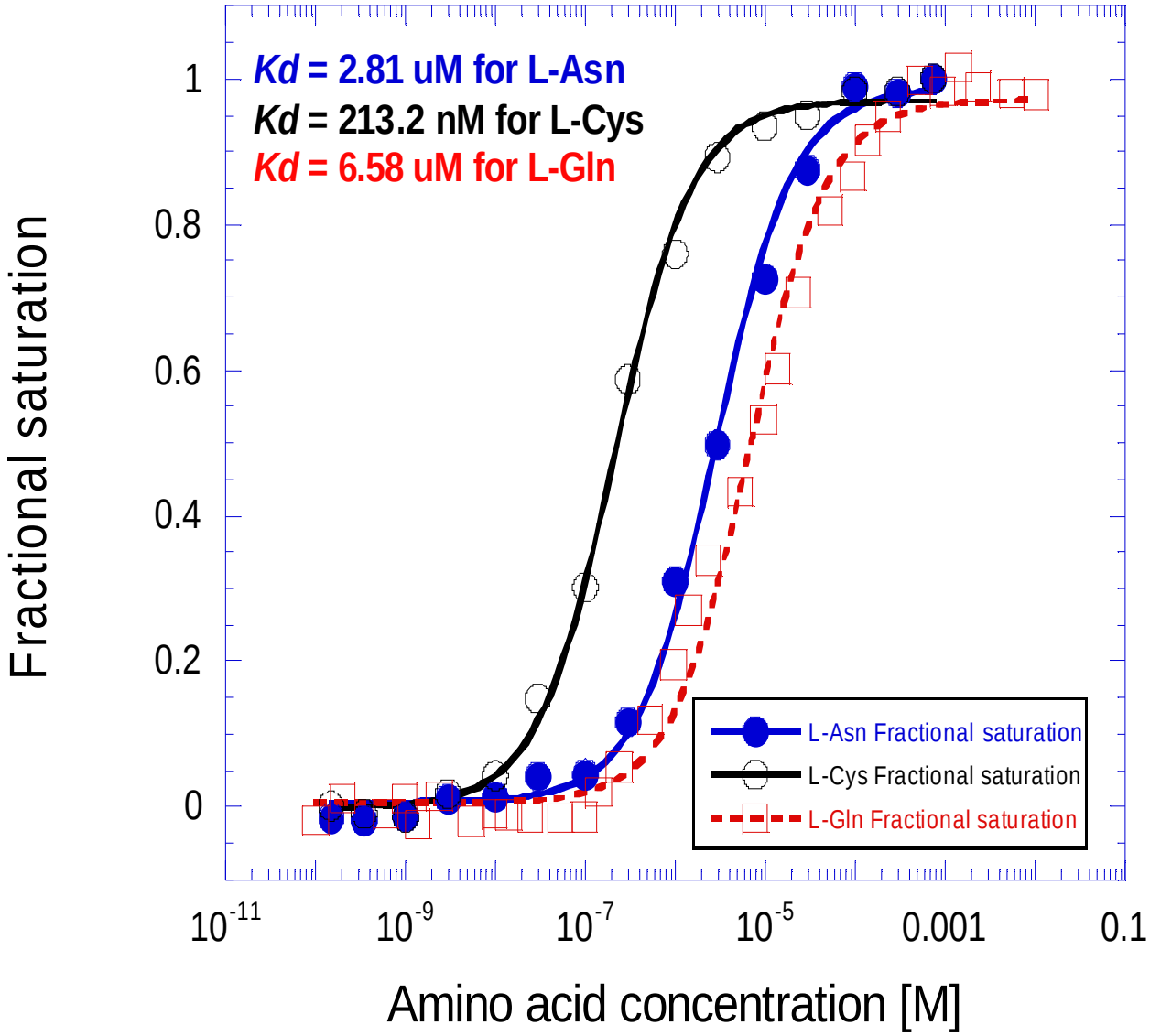

Fig. 12. Fluorimetric titration of FRET-based LIVBP sensor with L-Asn (●), L-Cys (o) and L-Gln (□). The lines shown are the best-fit binding curves for the respective ligands.

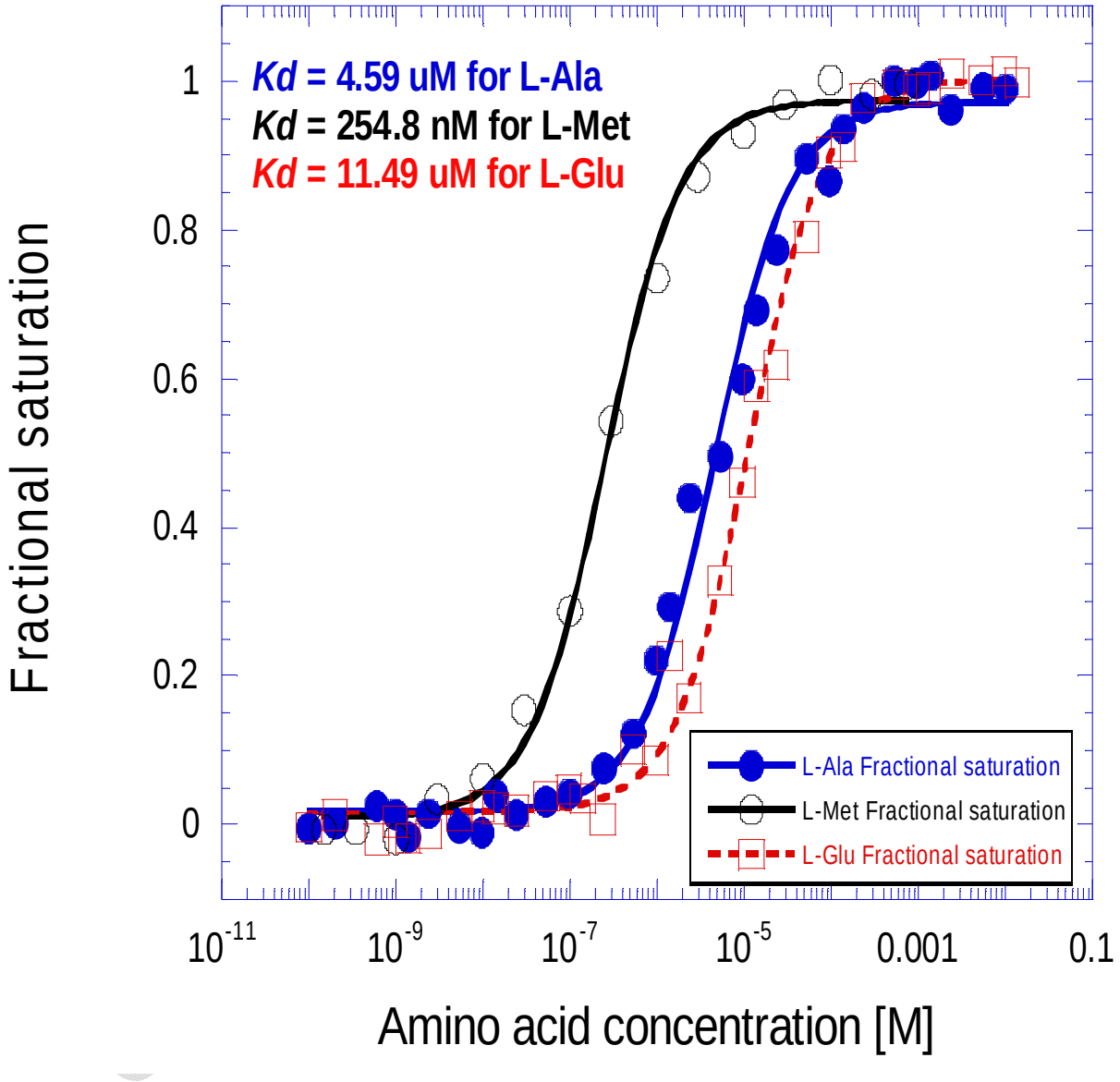

Fig. 13. Fluorimetric titration of labeled LIVBP-F118C with L-Ala (●), L-Met (o) and L-Glu (□). The lines shown are the best-fit binding curves for each ligand.